Excitation Spectra and Stokes Shift Measurements of Single Organic Dyes at Room Temperature

Martijn H.W. Stopel[†], Christian Blum[*,†], and Vinod Subramaniam[*,†,‡,§]

[†]Nanobiophysics, MESA+ Institute for Nanotechnology, University of Twente, P.O. Box 217, 7500 AE Enschede, The Netherlands

[‡]Nanobiophysics, MIRA Institute for Biomedical Technology and Technical Medicine, University of Twente, P.O. Box 217, 7500 AE Enschede, The Netherlands

[§]FOM Institute AMOLF, Science Park 104, 1098 XG Amsterdam, The Netherlands

Corresponding Authors

Christian Blum: c.blum@utwente.nl; Vinod Subramaniam: subramaniam@amolf.nl

Supporting Information

Experimental details

Sample preparation

To prepare our samples we diluted the perylene derivative N,N-di-(tert-butoxycarbonyl)-9-amino-N-(2,6-diisopropylphenyl)perylene-3,4-dicarboximide in a solution of 0.8 g polystyrene (PS) in 100 ml of toluene to achieve relevant single emitter concentrations (~1 nM). This dilution is spin-coated onto a clean coverslip for 10 seconds at 6000 rpm to immobilize the emitters in a PS polymer matrix. The coverslip was cleaned beforehand with an ozone cleaner *(UV/Ozone ProCleaner Plus, Bioforce, San Diego, CA)* for at least one hour.

Experimental procedure

We raster scan the sample with a custom-built single molecule fluorescence setup as explained in detail in reference 1 to localize the single isolated emitters. All experiments are performed at room temperature. We use an excitation wavelength of 510 nm and an intensity of approximately 1 kW/cm^2 at the diffraction limited focus spot, and integrate 10 ms per pixel to collect emission from the single perylene dyes across a 10x10 μm^2 area. The perylene dyes typically show a stable emission pattern with a sparse amount of blinking (not shown). After locating the single emitters, we select the ones that are fully spatially isolated and record both the excitation and emission spectra at the same location. To do so, we use two filter sets that can be interchanged in-between the spectral recordings. To measure excitation spectra we use an SP01-561RU filter in combination with LP02-561RU and FF01-582/15 filters (all filters from Semrock Inc., NY, USA) and excite the emitters using a wavelength scanning range from 461 nm to 561 nm (2.2 eV to 2.75 eV). The excitation spectra are recorded as a series of total emission intensity measurements with 200 ms integration time each, for each excitation wavelength. The excitation wavelengths are tuned using an acousto-optical tunable filter (AOTF, Crystal Technologies, West Chester PA, USA) to select any desirable wavelength in the

visible spectral band from a supercontinuum laser source (SC400-PP, Fianium Inc, UK). To measure emission spectra we use an FF02-447/60 filter in combination with a BLP01-488R long-pass filter (Semrock Inc., NY, USA and excite the emitters at a wavelength of 470 nm, and record the emission from ~500 nm and longer wavelengths (<2.5 eV), using a custom-built prism spectrograph that is equipped with an Andor Newton 971-BV camera (Andor Technology Ltd., UK). The filter sets ensure that excitation and emission light are fully isolated from each other and do not hinder the detection of the emission light coming from the single emitters.
After recording the spectra, we correct the emission spectra for background (recorded at areas between the single emitters). The excitation spectra are also corrected for background (recorded at areas between the single emitters). In addition we apply a photon flux density correction,

$$\Phi_d = \frac{P}{E_{ph} \cdot A} \sim \frac{P(\lambda)}{\lambda}$$

where Φ_d is the photon flux density, P the power at wavelength λ, E_{ph} the energy of a photon and A the area of the diffraction-limited focus spot. We did not correct for wavelength dependent differences in the sensitivity of the setup, which explain some of the differences in the spectral shape of the bulk emission spectra and the single molecule spectra.

Statistical analysis

Normality tests

Both excitation and emission peak energy distributions appear normally distributed, which we would expect, since random fluctuations of molecular properties cause spectral variations that are typically characterized by a normal distribution of the observed quantity.[2] As an additional test, we apply a Shapiro-Wilk (S-W) normality test to both distributions. The S-W test specifically suitable for small sample sizes ($n \leq 50$), but can also range up to $n = 2000$.[3] Generally, a p-value < 0.05 for the tested distribution is considered as a proof that the distribution is significantly different from a normal distribution while a p-value of 1 indicates a perfect match with a normal distribution.[4] For the distribution of excitation peak energies we find a p-value of 0.35 and for the distribution of the emission peak energies a p-value of 0.63, meaning that the S-W test does not consider both distributions to significantly differ from a normal distribution.

The Stokes shift histogram does not appear to be normally distributed. Therefore, we perform a S-W normality test on the Stokes shift distribution, which gives a p-value of 0.002, showing that the Stokes shift distribution is significantly different from a normal distribution.

Statistical analysis of the Stokes shifts

Interestingly, if we analyze the Stokes shifts using a k-means cluster analysis,[5] a good agreement is found with the Stokes shift histogram when having three statistically distinguishable groups. The mean Stokes shifts of those three groups are 96±12meV, 142±12meV and 198±20meV (standard deviation), which matches the peak locations energies and peak widths in Figure 3c. In addition, we select the data points in Figure 3b that correspond to these groups and determine the linear correlation coefficient (Pearson's coefficient) of the data points within each group. We observe a strongly increased correlation between the excitation and emission peak locations energies for the grouped datapoints ($r_1 = 0.95 \pm 0.02$, $N_1 = 29$; $r_2 = 0.93 \pm 0.05$, $N_2 = 21$; $r_3 = 0.85 \pm 0.10$, $N_2 = 9$), compared to that of all datapoints taken together ($r_{all} = 0.59 \pm 0.08$, $N_{all} = 59$), even though the statistical sample

decreases. The correlation coefficient errors (bootstrapped[6], see Figure S1) of the first two groups also become smaller after subdivision, supporting the increased correlation of the selected datapoints for the two most prominent peaks in the Stokes shift histogram.

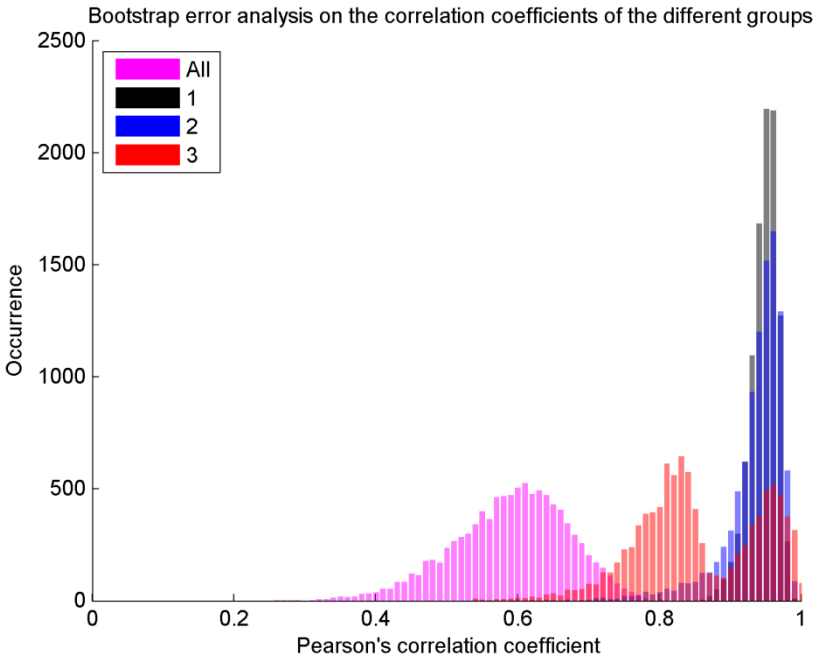

Figure S1. Bootstrap error analysis on the correlation coefficients of the different groups. After grouping the datapoints according to the selection found by the k-means cluster analysis, the correlation coefficient strongly increases and the error becomes smaller, even though the statistical sample decreases.

Additional bulk spectra

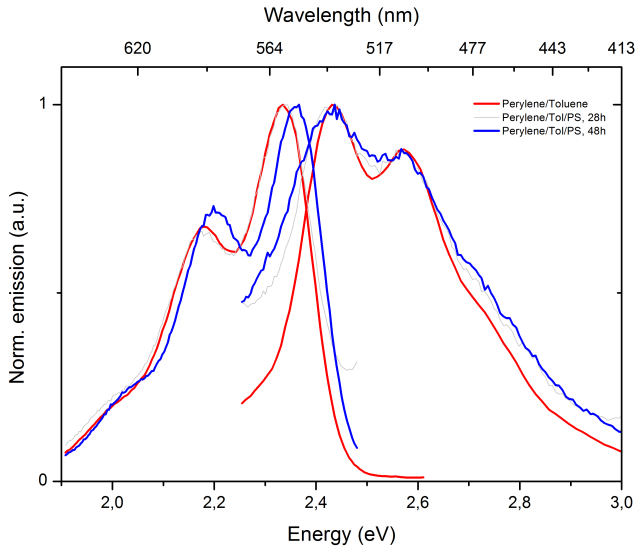

Figure S2. Additional bulk spectra of high concentration perylene in a thick layer of polystyrene upon drying of the layer.

Stokes shift as a function of the excitation maximum

For positive solvatochromism one would expect that the red shift of the excitation maximum is accompanied by an increase of the Stokes shift. We therefore plotted the Stokes shift as a function of the excitation maximum (see Figure S3 below). Interestingly we do not find the clear correlation between excitation maximum and Stokes shift that would be indicative of differences in the local polarity causing the differences in Stokes shift. It is hence likely that differences in the local flexibility give rise to the observed differences in the Stokes shift. A nanoenvironment that does not allow for reorientation to accommodate the changes of the dipole moment in the excited state will give rise to a smaller Stokes shift than a nanoenvironment that allows reorientation.

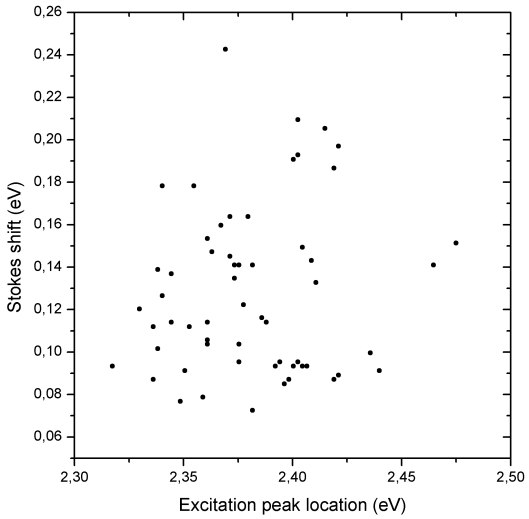

Figure S3. Scatterplots where Stokes shift is plotted versus excitation peak energies. There is no clear correlation between Stokes shift and excitation peak energy.

References

1. Blum, C.; Schleifenbaum, F.; Stopel, M.; Peter, S.; Sackrow, M.; Subramaniam, V.; Meixner, A. J. Room temperature excitation spectroscopy of single quantum dots. *Beilstein J. Nanotechnol.* **2011,** *2*, 516-524.
2. Blum, C.; Stracke, F.; Becker, S.; Mullen, K.; Meixner, A. J. Discrimination and interpretation of spectral phenomena by room-temperature single-molecule spectroscopy. *J. Phys. Chem. A* **2001,** *105*, 6983-6990.
3. Royston, J. P. An Extension of Shapiro and Wilk's W Test for Normality to Large Samples. *J. R. Stat. Soc. C* **1982,** *31*, 115-124.
4. Fisher, R. A. *Statistical Methods for Research Workers*. 1925.
5. Hartigan, J. A.; Wong, M. A. Algorithm AS 136: A K-Means Clustering Algorithm. *J. R. Stat. Soc. C* **1979,** *28*, 100-108.
6. Efron, B. Nonparametric Estimates of Standard Error: The Jackknife, the Bootstrap and Other Methods. *Biometrika* **1981,** *68*, 589-599.